*MRS Communications (2023) 13:928–941*

https://doi.org/10.1557/s43579-023-00411-9

MRS Communications

Early Career Materials Researcher Prospective

# The art of peer pressure between nanocrystals: High-pressure surface nanochemistry

**Yasutaka Nagaoka, Peter Saghy, Ou Chen,** Chemistry Department, Brown University, Providence, RI, USA

Address all correspondence to Yasutaka Nagaoka at **yasutaka_nagaoka@brown.edu**

(Received 4 April 2023; accepted 27 July 2023; published online: 8 August 2023)

## Abstract

Pressure creates precious materials; diamonds are produced in the Earth's core–mantle, and ammonia is synthesized by the Haber–Bosch process. Recent research has demonstrated that applying high pressure to aggregates of nanocrystals can lead to a distinct interplay between them, resulting in novel nanostructured materials previously thought to be impossible. Examples of such materials include nanograin-boundary materials, 1D–2D nanomaterials fused from 0D nanocrystals, and materials that can maintain a high-pressure crystal phase at ambient pressure. This article showcases cutting-edge research emphasizing the importance of surfaces, i.e., high-pressure surface nanochemistry. We also discuss the challenges and prospects in this field.

## Introduction

"No pressure, no diamond". This quote by Thomas Carlyle has been proven to be scientifically correct:[1–3] a recent study accurately depicts a graphene-diamond phase transition at c.a. 1500°C and 20 GPa.[1] As such, pressure is a primitive parameter used to tune materials' properties and thermodynamics, i.e., Gibbs'-free energy equation, $G=E+PV-TS$. Under high pressure, a number of materials exist in alternative, high-pressure phases different from their phases under ambient conditions. These high-pressure phases can show superior properties, such as optical,[4,5] mechanical,[6] energy,[7,8] thermal conductivity,[9] and electronic properties.[10] One of the most promising materials in this field is high critical-temperature superconductors.[11,12] Drozdov et al. reported that $LaH_{10}$ exhibited superconductivity at 250 K under 170 GPa,[11] and FeSe reported by Chu et al. showed a significantly higher critical temperature of 37 K under 4.2 GPa than 9.3 K at ambient pressure.[12] Furthermore, materials under high pressure can also exhibit fundamentally unique properties: pressure can shorten bond distances in a molecule, which affects molecular orbitals, resulting in exotic chemical bonds.[13] For example, super-heavy element compounds were recently found to exhibit increased covalency under high pressures.[14,15] The discovery can help us better understand the behavior of underground nuclear waste.[14,15]

Despite these exciting discoveries, some research conducted under extreme conditions may be considered less practical. For example, when a property that emerges at 10 GPa is used for a device with a size of 1 $cm^2$, the continuous application of a force of 1000 tons is required (which is equivalent to the weight of a cruise ship!). However, several recent reports suggest that these issues could be circumvented in some cases. In the case of FeSe, the crystal takes a tetragonal-based structure at ambient pressure and an orthorhombic-based structure at a pressure greater than approximately c.a. 1.9 GPa exhibiting a high critical temperature for superconductivity.[12] Interestingly, the high-pressure phase of FeSe could be preserved for at least 7 days after releasing pressure at room temperature.[12] Obviously, higher stability is required for practical use. The detailed general mechanism for better high-pressure phase maintenance has not yet been clarified, but this result indicates high-pressure phase materials could be potentially used in normal conditions.

High-pressure nanochemistry combined with nanocrystal surface engineering could address the instability issues of materials with high-pressure phases.[16,17] For example, Cao et al. demonstrated that preserving high-pressure phases at ambient pressure can be achieved with adequate engineering of nanocrystals and using a suitable pressure process.[17] With this methodology, high-pressure phases of CdS and CdSe can be preserved for as long as 7 years.[17] Likewise, recent discoveries in the high-pressure surface nanochemistry enable one to produce novel nanostructured materials previously thought to be impossible.[16] Essentially, the controlled jamming and effective interaction between nanocrystals under high pressure is the key. In this perspective article, we discuss novel materials that have been created from nanocrystal aggregates by high-pressure processes, especially highlighting the importance of the surface.

This article is structured as follows. First, we briefly introduce the basics of high-pressure chemistry, including experimental setups and materials' response to pressure (i.e., hydrostatic vs. non-hydrostatic). Then, we provide an overview of early pioneering works in high-pressure nanochemistry. Following that, we introduce the latest research on nanocrystal assemblies under high pressure. The materials produced in this field include 1D materials, such as nanorods and nanowires, and 2D materials, such as nanoplatelets, achieved through a

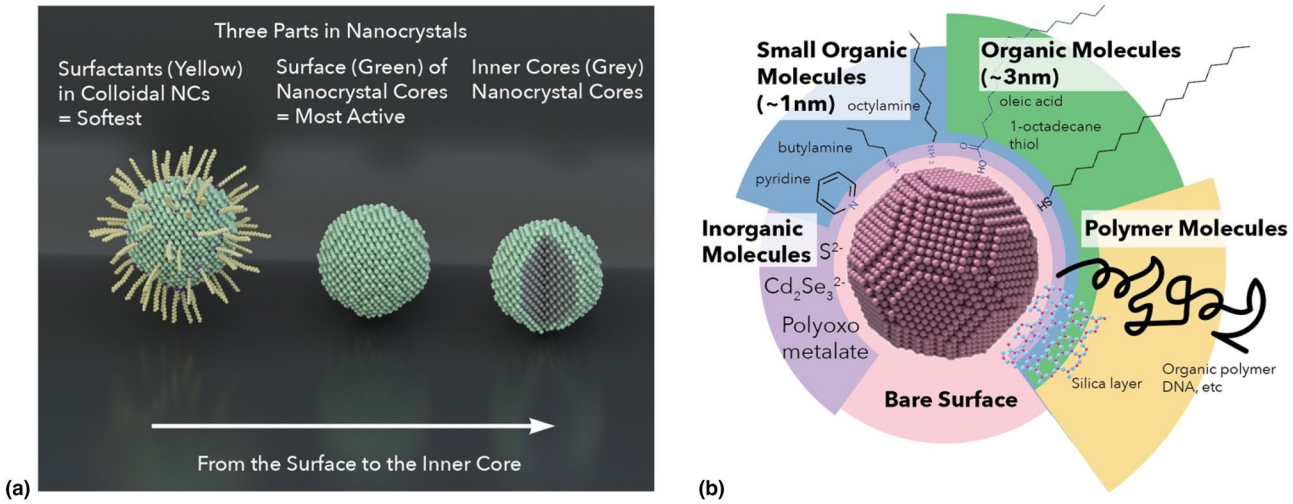


**Figure 1.** (a) Three parts in nanocrystals: surfactants capping the nanocrystals' inorganic core (yellow parts in the left model), the surface of the nanocrystals' inorganic core (pale green in the center model), and the inner core of the nanocrystals (grey in the right model). (b) Surface engineering of nanocrystals. Nanocrystals can host various molecules on the surface.

directional fusion of nanocrystals. Additionally, researchers have created nano-grain boundary materials using nanocrystals as building blocks. Moreover, materials with a high-pressure phase that can stably exist at ambient conditions for years will be discussed. Next, we discuss challenges related to characterizing these materials and fundamental questions regarding the surface chemistry of nanocrystals under high-pressure conditions. Finally, we provide our perspective on this highly promising research topic. We aim to attract the attention of researchers from various disciplines, as this emerging research area has the potential to bring a bigstepper to a new class of materials science.

## A hierarchy of responses to pressure in nanocrystals

High-pressure nanochemistry research is unique compared to conventional high-pressure experiments because nanocrystals have three distinct areas with different mechanical properties and reactivities that concurrently respond to applied pressure. Figure 1(a) illustrates the three different areas: the surfactant, the surface of the inorganic core, and the inner core of the nanocrystal inorganic core [from left to right in Fig. 1(a)]. Typical nanocrystals are capped by hydrocarbon-chain-based molecules with a length of 2–3 nm [yellow parts in Fig. 1(a) left]. Such organic surfactants are the softest part of the nanocrystals. As a rule of thumb, under pressure, the softest materials and the weakest bonds are squeezed first.[13] Thus surfactants are compressed foremost in nanocrystal aggregates.[13,16] The surface of the inorganic cores [pale green atoms in Fig. 1(a) middle] is the first line of interaction when nanocrystal cores physically interact. Typically, the surface of the nanocrystals exhibits high energy, leading nanocrystal interactions/reactions. The inner part of the nanocrystal inorganic core is responsible for most of the nanocrystal atoms [gray atoms in Fig. 1(a) right]. Most measurements result from this part, such as X-ray diffraction (XRD), transmission electron microscopy (TEM), etc.

Nanocrystals can offer a variety of surface states. Exposing crystal facets can be controlled by synthesizing differently shaped nanocrystals, which makes nanocrystals attractive research subjects for surface chemistry.[18] Additionally, nanocrystals can host a variety of surfactant molecules, including organic molecules, biomolecules, and functional inorganic clusters [see Fig. 1(b)].[19–22] While previous high-pressure nanocrystal experiments have only used a limited number of surfactants,[16] there are many options for scientific exploration.

## Pressure apparatus and pressure medium

This section briefly explains the pressure apparatus typically used in pressure experiments: Diamond Anvil Cells (DACs) and piston-cylinder presses. We also briefly discuss pressure media and the resulting hydrostatic and non-hydrostatic pressure environments.

### *Pressure apparatus*

Pressure generates by exerting force on the area of interest. Generating pressure is generally calculated with the equation;

$$P = F/A$$

where P, F, and A are pressure, force, and area, respectively.

#### *Diamond anvil cell*[23]

Figure 2(a) and (b) show a schematic illustration and a photograph of a DAC. A DAC consists of a pair of diamonds, and samples are placed in a hole in a gasket between the two diamonds.[23,24] Diamonds are known to be the hardest materials,

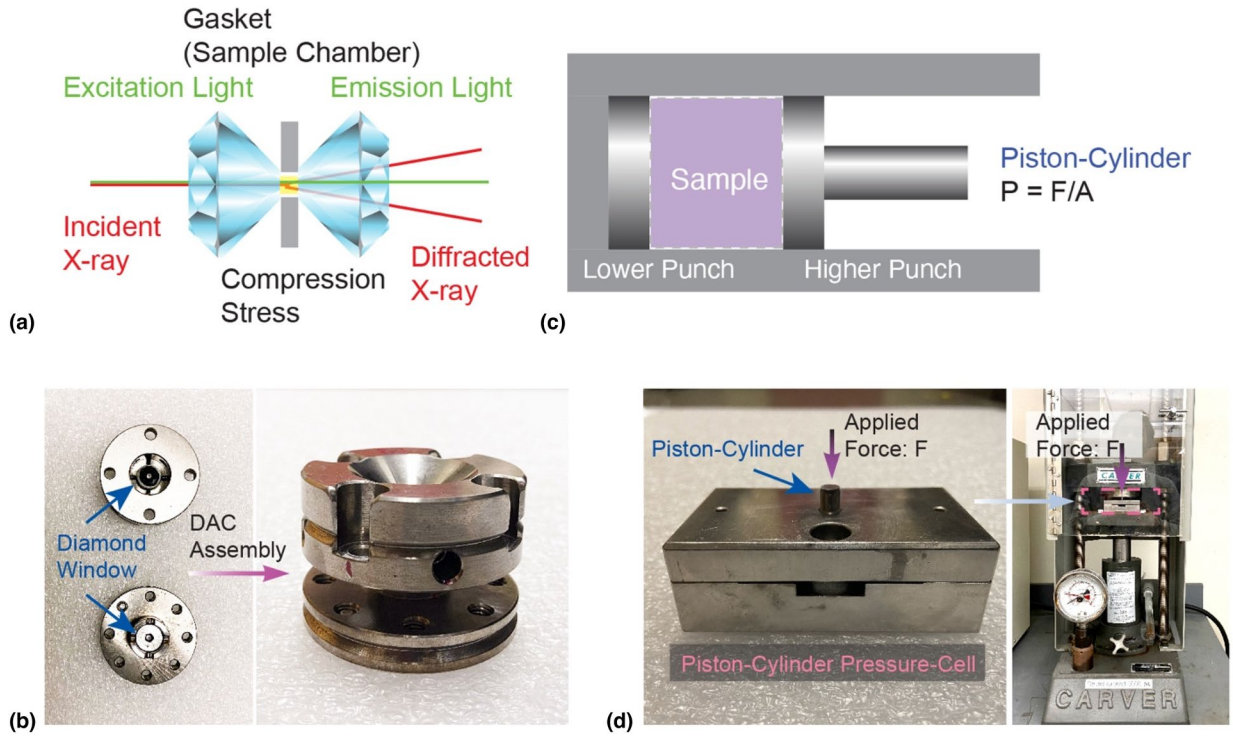


**Figure 2.** Pressure apparatus: (a) Schematic illustration and (b) a photograph of a diamond anvil cell. (c) Schematic illustration and (d) a photograph of a piston-cylinder pressure cell.

with a Mohs hardness value of 10, and can withstand huge applied forces. The applied pressure typically ranges from 0.1 to 200 GPa and is monitored using a chip of ruby which exhibits a pressure-dependent fluorescence peak position.[25]

Using a DAC, it is possible to conduct *in-situ* spectroscopic measurements through the diamond windows [Fig. 2(a)].[16] These measurements include X-ray scattering, Raman spectrum, absorption, and fluorescent spectroscopy.[16] Combining these techniques enables the mapping of the complete structural-property relationships of materials under pressurized conditions.[26,27]

### Piston-cylinder press

Figure 2(c) shows a schematic cartoon of a piston-cylinder press. A piston press consists of upper and lower punches and samples are placed between them. Forces are applied using a press [shown in Fig. 2(d)], and pressure is calculated by dividing the applied force by the area of the piston-cylinders. The applicable pressure is dependent on the materials of the piston-cylinders. While pistons made of steel with Mohs hardness values of 4–5 can withstand no more than 1 GPa,[28] state-of-the-art piston-cylinders can withstand pressures as high as 3–7 GPa.[29] Compared to DACs, piston-cylinder presses can handle larger sample quantities. These setups are commercially available as IR pellet makers with heating functions and are technically similar to some powder metallurgy processing.[30]

## Pressure medium and pressure propagation: hydrostatic pressure vs. deviatoric stress

A pressure medium can be placed in the sample chamber in pressure experiments. Commonly used pressure media include noble gases such as Ne and Ar,[25] as well as inert solvents such as an ethanol-methanol mixture and silicon oils.[16] These pressure media serve as pressure pathways that ensure a uniform hydrostatic pressure environment.

When pressure is applied without a pressure medium or when the pressure medium is solidified under high pressure, pressure propagation becomes significantly inhomogeneous, creating a non-hydrostatic pressure environment.[16,31] Interestingly, non-hydrostatic pressure can have beneficial effects on materials for some emerging phenomena.[16,31] Indeed, many of experiments introduced in this perspective article were done without a pressure medium. It should be noted that reliable results from high-pressure experiments in the absence of a pressure medium require firm confirmation of reproducibility and statistical validation throughout the sample area, considering possible significant inhomogeneous pressure propagation.

Figure 3(a) illustrates materials' mechanical transformation in response to pressure,[32] assessing response in each dimension (i.e., in the x (L: length), y (W: width), and z (H: height) directions), which defined as dL, dH, and dW [Fig. 3(a)].[32] When pressure is hydrostatic, materials feel isotropic compressive stress, so the resulting deformation is expressed as

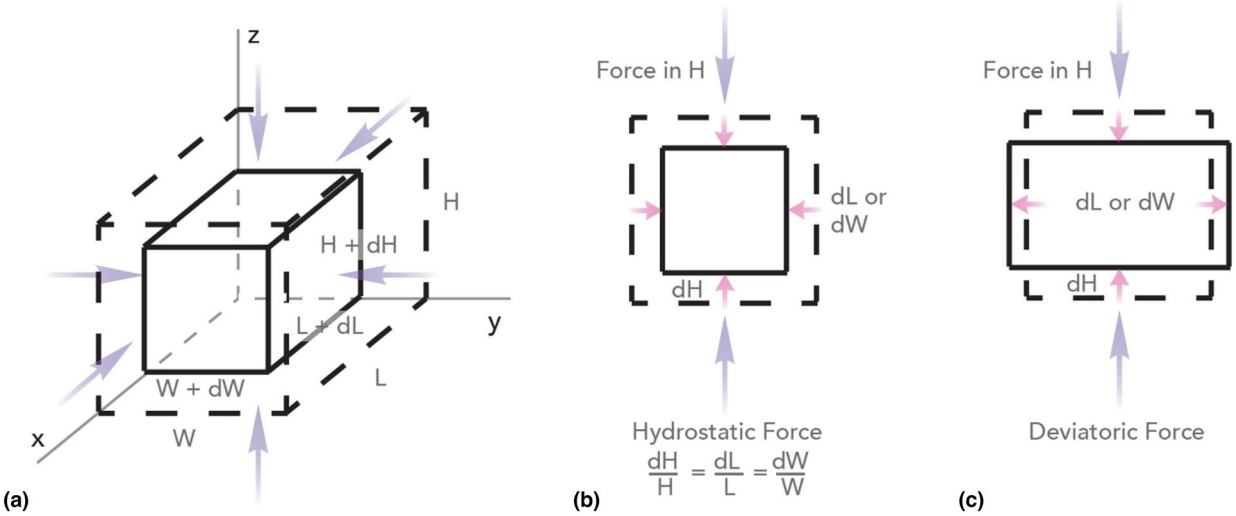


**Figure 3.** Transformation under pressure. (a) Deformation in response to forces in the x (L: length), y (W: width), and z (H: height) axes. (b, c) Schematic of hydrostatic (b) and deviatoric (c) forces exerting in the z (H: height) direction.

*dL/L = dH/H = dW/W* [Fig. 3(b)]. In contrast, when the ratios of dL/L, dH/H, and dW/W are not equal, the stress response is considered not hydrostatic. This is referred to as non-hydrostatic or quasi-hydrostatic pressure in some publication.

One possible cause of non-hydrostatic conditions is deviatoric stress.[33] Pressure can be deviated to generate strains in different directions from the pressure direction [Fig. 3(c)]. The deviated stress from the pressure direction is called deviatoric stress. In reality, the pressure response of materials is a convolution of both hydrostatic and deviatoric stress. Microscopically, pressure without pressure medium propagates through touching points of nanocrystals, i.e., force chains in granular materials.[34,35] As a result, pressure is effectively used for nanocrystals' physical interaction that may lead to special interplays.

## High-pressure nanochemistry: using an example of CdSe

A phase transition is one of the most dramatic chemical events that pressure can induce. In solid materials, when pressure exceeds a threshold where the atomic bond distance becomes too short, crystal structures undergo reorganization and form high-pressure phase crystal structures, resulting in a solid–solid phase transition.[32] Figure 4 illustrates the phase transition of bulk CdSe. Bulk CdSe takes on zinc-blende or wurtzite [Fig. 4(a) inset] structures as its most thermodynamically stable structure at ambient pressure.[36] Under increasing pressure, the lattice constant continuously shrinks, and above approximately 2.0 GPa, the crystal structure transforms into a rock-salt structure.[36] When releasing the pressure, backward phase transition happens at the phase transition pressure as the thermodynamics of CdSe dictates.[36]

Nanocrystals exhibit distinct dynamics in phase-transition processes compared to conventional bulk materials. Alivisatos' group conducted pioneering work demonstrating the size dependence of phase transition pressure.[37,38] Figure 4(b) depicts a plot of a high-pressure phase fraction of 1.8 nm CdSe nanocrystals over applied pressure.[37] The phase transition pressure was between 6.0 and 8.0 GPa, significantly higher than the bulk phase transition pressure of approximately 2.0 GPa.[37] During the pressure release process, the nanocrystals returned

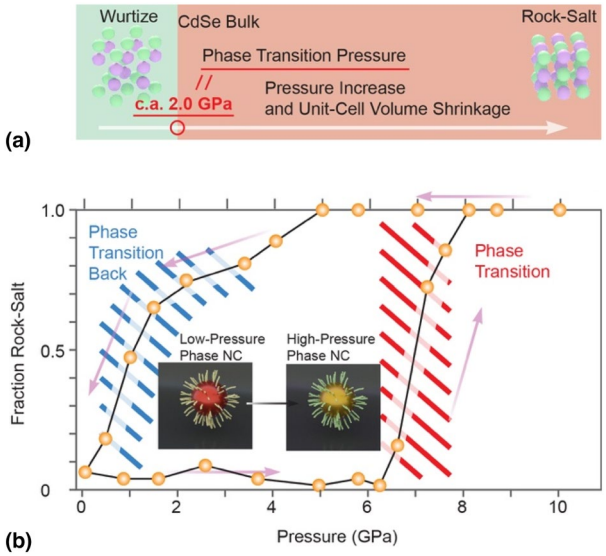


**Figure 4.** Phase transition of CdSe: (a) Phase diagram of CdSe crystal structure vs. applied pressure. Bulk CdSe takes zinc-blend or wurtzite structure under less than c.a. 2.0 GPa and rock-salt structure under more than c.a. 2.0 GPa. (b) Typical plot showing the fractions of high-pressure phase over applied pressure for CdSe nanocrystals. The phase-transition during a pressurizing process and the phase-transition back during a pressure-releasing process are highlighted with red and blue stripes, respectively. (b) was reproduced from Ref. 37.

to the ambient phase in the pressure range of 0–2.0 GPa. As a result, the plot exhibited a huge hysteresis loop [Fig. 4(b)]. The discrepancy between pressure responses of nano- and bulk-sized materials originates from phase-transition kinetics in nanosize crystal domains and thermodynamic effects led by the high surface areas of nanocrystals.[16,26,38,39]

## The art of peer pressure between nanocrystals: nanocrystal assemblies under high-pressure

This section highlights surface reactions between nanocrystals driven by high-pressure processes and explains the uniqueness of the resulting materials. Specifically, we discuss how nanocrystal surface engineering can control the nanocrystals' pressure response, the interaction between nanocrystals during high-pressure processes, and the consequences. For this discussion, we use three leading-edge nanostructured materials created with methodologies based on the high-pressure surface nanochemistry: pressure-sintered 1D or 2D materials (Fig. 5), nanosized grain-boundary materials (Fig. 6), and high-pressure phase materials (Fig. 7).

### *Pressure-sintered 1D/2D materials*

By applying high pressure (c.a. 10–20 GPa) to nanocrystal superlattices (ordered arrays of nanocrystals), the nanocrystals can fuse along the pressure directions. As a result, long nanowires and nanoplatelets with a high aspect ratio (i.e. the

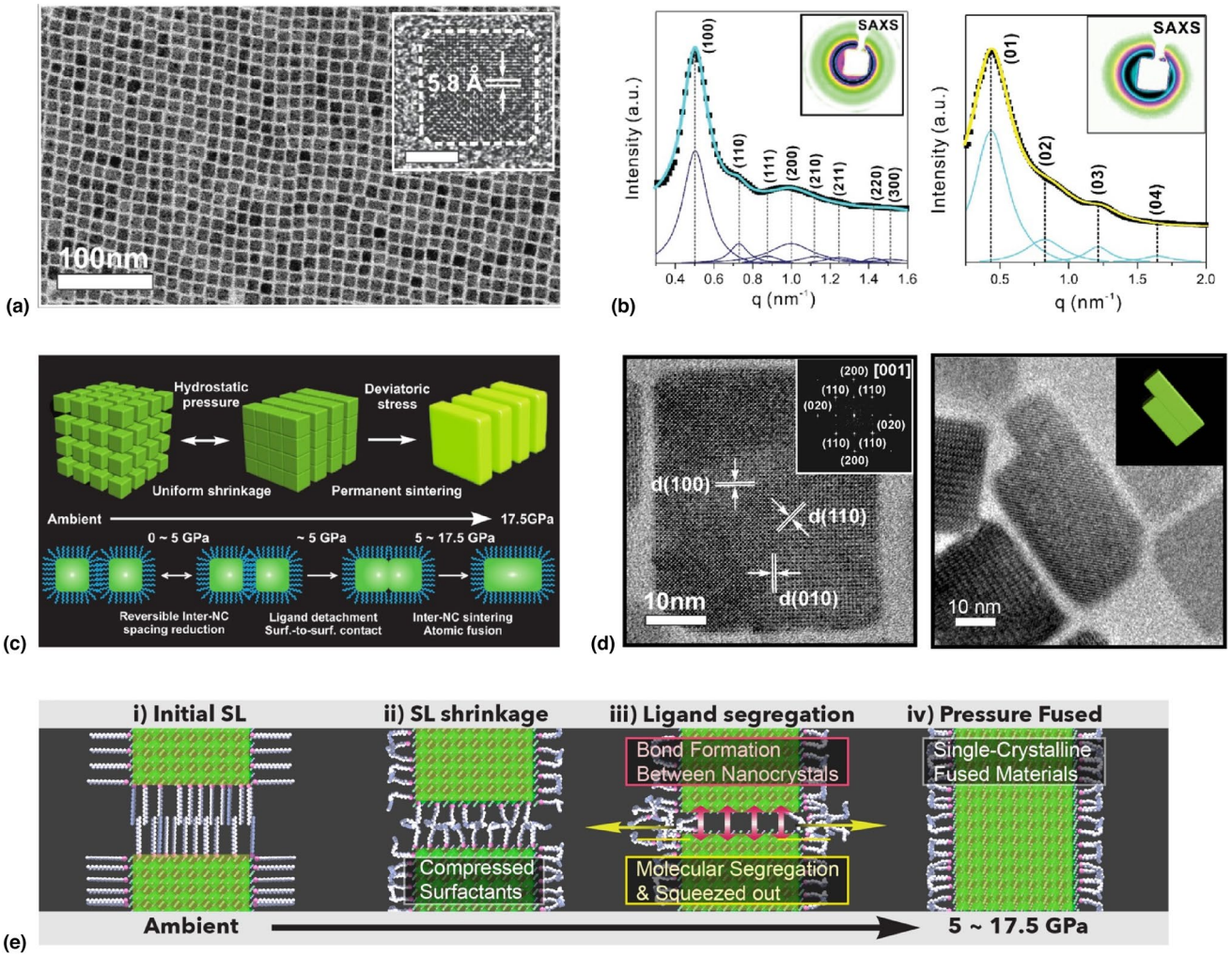


**Figure 5.** Pressure-driven nanocrystals fusion into 2D materials in superlattices. (a) TEM images of 10.2 nm $CsPbBr_3$ nanocubes and the high-resolution TEM (inset). These nanocrystals were used for nanocrystal superlattices. (b) SAXS spectra of before (left) and after (right) a 17.5 GPa pressurizing process, showing simple-cubic and lamellar superstructures respectively. The inset panels show 2D SAXS patterns. (c) Schematic presentation of the pressure-driven nanocrystal fusion into 2D materials. (d) TEM images of the resulting nanoplatelets from fused $CsPbBr_3$ nanocrystals showing seamless single crystallinity. The inset panels show the fast Fourier transform pattern of the nanoplatelet (left) and corresponding computer model (right). (e) Schematics of the pressure-driven nanocrystal fusion highlighting the surface reactions of the $CsPbBr_3$ nanocubes. (a–d) were reproduced from Ref. 26.

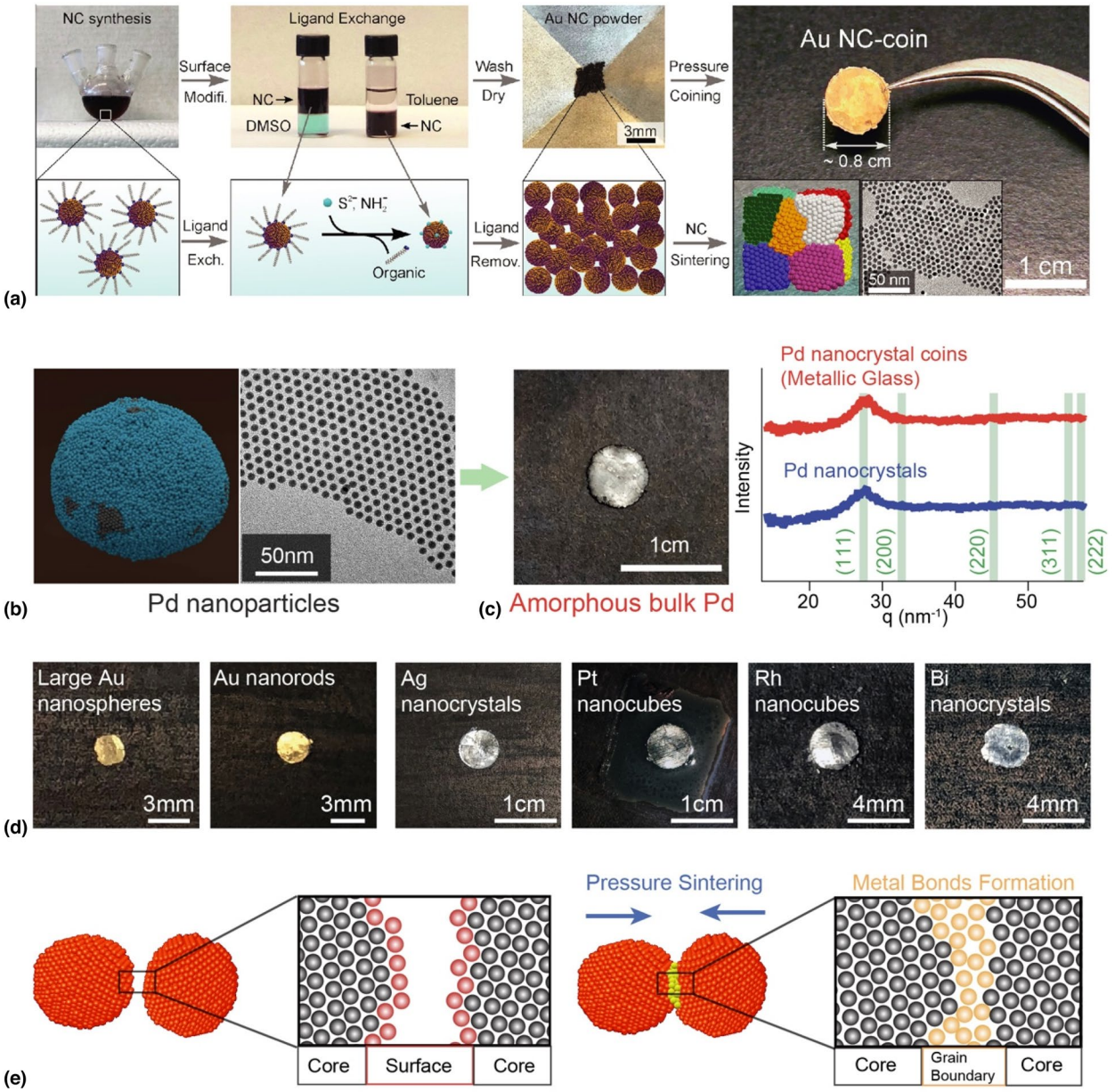


**Figure 6.** Nanocrystal coining method. (a) Step-by-step procedure using 6.5-nm gold nanocrystals. First, uniform colloidal nanocrystals were synthesized (left). Then, the nanocrystals underwent chemical surface modifications, and the surfactant was replaced by small inorganic surfactants (center-left). Subsequently, the nanocrystals were washed multiple times to remove the inorganic surfactants, and nanocrystal powders were obtained by a complete dry process (center-right). The powder was compressed under approximately 0.6 GPa with a piston-cylinder cell, which turned the black powder into golden coin-shaped bulk materials. (b) Palladium nanoparticle with amorphous atomic structures (left). 3D atomic tomography of the palladium nanoparticles (right) and low-magnification TEM image. (c) Amorphous palladium coin (left) photograph (right) XRD spectrum before and after the nanocrystal coining process showing there is no crystallinities. (d) Nanocrystal coin collection: nanocrystal coins from gold nanospheres (61 nm), gold nanorods (40-nm width and 111-nm length), silver nanospheres (9.5 nm), platinum nanocubes (8.4 nm), rhodium nanocubes (7.3 nm), and bismuth nanospheres (18.9 nm) (from left to right). (e) Schematic illustration of metal bond formation during the nanocrystal coining method. (a–d) were reproduced from Refs. 28 and 55.

aspect ratio: 5~>200) have been produced with a wide range of components including semiconductors (e.g., CdSe, PbS, PbSe, perovskite)[26,40–43] and metals (e.g., Ag, Au).[33,44,45] Figure 5(a–d) presents the stepwise procedure using an example of $CsPbBr_3$ nanocrystal superlattices.[26] Uniform 10.2 nm $CsPbBr_3$ nanocubes were synthesized and used as building blocks of the nanocrystal superlattices [Fig. 5(a)]. The nanocubes formed simple-cubic superlattices and were pressurized under 17.5 GPa. The superstructural change was monitored using small angle X-ray scattering measurements

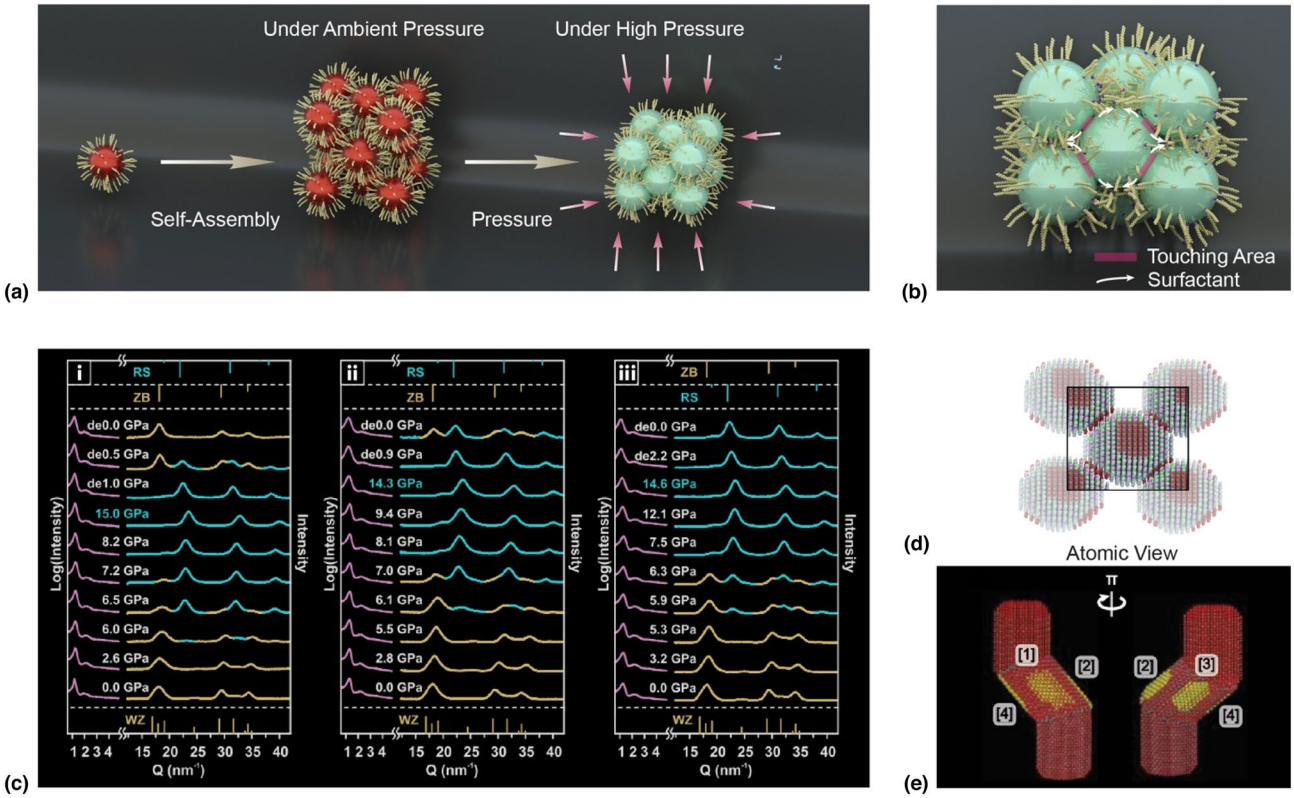


**Figure 7.** High-pressure phases preserved through nanocrystal network formation. (a, b) Schematic illustration of the process. (a) Nanocrystals, capped with adequate surfactants (left), are self-assembled into superlattices (center). The nanocrystals were then put under high pressure (right). Under the pressure, the nanocrystals underwent a phase transition, and the nanocrystal superlattices transformed into deformed superstructures. (b) The nanocrystals were in contact in multiple places (highlighted in red) in the pressurized superstructures after releasing the pressure. (c) WAXS and SAXS patterns were collected during compression and decompression at different pressures. CdSe NCs were functionalized with octylamine of (i) 92% surface coverage, (ii) 62% surface coverage, and (iii) capped with a mixture of octylamine and CTAB (with a molar ratio of 5:1) of 63% surface coverage in terms of hydrocarbon chains. (d, e) Atomic models of spherical CdSe (d) and CdSe@CdS nanorods (e) after the pressurizing process. The touching areas are highlighted in red and yellow, respectively. (c) and (e) were reproduced from Ref. 17.

(SAXS) [Fig. 5(b)], showing that a simple cubic superstructure [Fig. 5(b left)] turned into a lamellar [Fig. 5(b right)] through the pressurizing process. This resulted from a pressure-driven fusion between nanocubes in the superlattices, as depicted in Fig. 5(c). The fused nanocubes became a single-crystalline nanoplatelet which was presented in Fig. 5(d).

## The significance

Pressure-sintering is a clean method that does not require expensive settings.[16] Furthermore, this process can be robustly applied to a variety of components to produce low-dimensional materials. While colloidal chemistry has produced a wide range of uniform nanomaterials,[46] the synthesis of anisotropic nanomaterials typically relies on crystallization kinetics during the synthesis.[46] This is inherently limited by the crystal structure, which imposes limitations on the resulting morphologies and components. Pressure-sintering can circumvent the problem and be robustly applied to a variety of components, including metals, quantum dots, and perovskite materials,[47] and can produce 1D and 2D nanomaterials with extremely uniform thickness inherited from the uniform building block nanocrystals. This is important because morphologies are the primary factors that determine the properties of nanocrystals. In particular, 1D and 2D nanomaterials are highly sought after for their applications in biomarkers and nanoelectronics.[47]

Compared to other sintering processes, pressure sintering is exceptional in its ability to preserve the size of the original nanocrystals in the thickness of resulting materials.[16,33,41] Typical heat sintering, ripening, and coalescent processes involve atomic movements of entire materials, causing the morphologies of materials to change completely.[48] In contrast, pressure sintering of nanocrystals mainly involves the first several outermost atomic layers of nanocrystal cores, allowing the shape of the original nanocrystals to be preserved in directions that nanocrystal fusion did not occur in.[28,33]

### The surfactant

Figure 5(e) presents how the surfactants move during the pressure-driven nanocrystal fusion. As formed, nanocrystal superlattices have surfactants touching each other between neighboring nanocrystals [Fig. 5(e–i)]. Under pressure, surfactant molecules are compressed first, making isotropic compression in nanocrystal superlattices [Fig. 5(e–ii)]. Upon further pressure, surfactant molecules are dissociated from nanocrystal surfaces and are pushed away from the space between nanocrystals [Fig. 5(e–iii)]. The dissociation process requires significant energy to break the bond. For example, gold nanocrystals capped by 1-dodecanthiol, which is also known to make nanocrystal fusion in superlattice under high pressure,[33,44,45] have a bond energy estimated as 1.3–1.6 eV.[49] It is important to note that the deviatoric stress is the main driving force of the dissociation process occur.[33] Wang et al. reported PbS nanocrystals fused to form nanosheets under 14.5 GPa in absence of pressure medium.[50] Meanwhile, Shevchenko et al. reported a series of nanocrystal superlattice behaviors under high pressure in a DAC with Ar as the pressure medium, which provides highly hydrostatic pressure conditions.[51] In the report, a single-crystalline PbS nanocrystal superlattice kept shrinking uniformly until 55 GPa without any evidence of nanocrystal fusions.[51] Lastly, another important role of nanocrystal surfactants is to serve as templates for nanocrystal fusions. After surface segregation processes [Fig. 5(e–iii, iv)], the segregated surfactants prevent nanocrystal fusion in unwanted directions.

### The reaction at the surface of nanocrystals

After segregating surfactants from nanocrystals, a fusion of nanocrystals can occur, resulting in materials with new morphologies [see Fig. 5(c and d step-iii)]. This fusion process relies on surface reactions between neighboring nanocrystals to generate new chemical bonds [highlighted in red arrows in Fig. 5(d step-iii)]. According to previous reports, three types of bonds can be formed during fusion: metal bonds, ionic bonds, and core–core physical touchings.[16] Depending on the bond, the grain-boundary conditions in the resulting materials will vary. When metal bonds are formed, materials with random crystal domains can be obtained. Fan group's series of reports on gold[44,45] and silver[52] nanowires fused from nanocrystals in superlattices clearly showed polycrystalline domains. In contrast, materials with ionic crystals tend to possess single crystallinity in the resulting materials from the pressure-sintered nanocrystals. Figure 5(b) shows an example of $CsPbBr_3$ nanoplatelets fused from nanocubes, with high-resolution TEM showing a large single-crystalline domain.[26] Ionic bonds are highly directional, defined by the crystal structure, and do not allow for arbitrary orientation of crystal domains in a material. Similar single crystalline materials resulting from pressure-fused nanocrystals include PbS[50,53] and PbSe.[53] Another consequence for ionic crystal nanocrystals is that they can be connected through core–core physical touchings. Fan et al. reported nanowires of CdSe nanocrystals with polycrystalline lattice domains by pressurizing CdSe nanocrystal superlattices.[41]

## Nanosized grain-boundary materials

Grain-boundary materials have designed crystal domains that exhibit desirable functions.[54] By controlling the size, shape, and interfacial conditions of the crystal domains, one can improve materials' mechanical, electrical, and thermal properties of grain-boundary materials.[28,54]

We have recently developed a unique method to produce grain-boundary materials called the "nanocrystal coining method."[28] Figure 6(a) shows the basic procedure: nanocrystals are synthesized [Fig. 6(a left)], and all surfactants are removed through surface modifications followed by extensive washing [Fig. 6(a middle left)]. The bare nanocrystals are completely dried under vacuum resulting in the formation of dry nanocrystal powders [Fig. 6(a middle right)], which are subsequently solidified with piston-cylinder cells under c.a. 0.6 GPa. The resulting 'coin' possesses materials integrity similar to bulk materials with characteristic metallic appearance [Fig. 6(a. right)].[28] Importantly, the original nanocrystal size [as seen in the TEM image in the left inset panel in Fig. 6(a right)] is preserved as the crystal domains in the resulting materials as depicted in the model in the center inset panel in Fig. 6(a) right. The nanosized grain-boundary condition originates the Hall–Petch effects enhancing the hardness values ($H_0$) of the materials, $H_0 = 0.65$ GPa for the gold nanocrystals coin (6.5 nm) vs. $H_0 = 0.3$ GPa for gold bulk materials.[28]

The advantage of this methodology is the ability to translate nanocrystals' properties into the resulting bulk materials.[28] As proof of concept, we have produced the first examples of single-component amorphous metals using palladium nanoparticles.[28] Palladium nanoparticles can take amorphous crystal structures with the assistance of surface energy.[55,56] However, bulk-sized single-component metals, including palladium, have too high a crystallization tendency to form amorphous structures under normal conditions. We applied the nanocrystal coining method to amorphous palladium nanocrystals, preserving amorphous atomic structures in the created bulk materials.[28] These bulk materials exhibited both a shiny metallic appearance originating from the surface polariton mode and high electric conductivity ($10^5$ A/m).[28]

### The significance

The nanocrystal coining method allows unprecedentedly precise and highly controllable grain-boundary engineering.[54] Colloidal nanocrystals provide a vast library of materials with various components, shapes, and sizes with sub-nanometer controllability.[18,57] The nanocrystal coining method can use these nanocrystals as direct building blocks for grain-boundary materials in a bottom-up fashion, which enables significantly

precise materials designs over conventional methods for producing grain-boundary materials.

By incorporating multiple kinds of nanocrystals or nanocrystals composed of multiple kinds of materials (i.e., core–shell nanocrystals), highly designed composite materials can be obtained such as solid dispersant composite materials.[58,59] Additionally, leaving a small amount of surfactant cluster-molecules on nanocrystals to the extent that it does not interrupt nanocrystal fusion in the consolidation process could work as controllable doping at the crystal-domain interface in the resulting materials.[16]

### The surfactant

The absence of surfactant is crucial for the nanocrystal coining method.[28] We found that an incomplete washing process, which leaves a significant amount of nanocrystal surfactants, results in failure in metallization after the coining process.

### The reaction at the surface of nanocrystals

The main reactions for the nanocrystal coining method involve metal bond formations at the nanocrystal surface [Fig. 6(e)]. Metal bonds are flexible in bonding direction, allowing for randomly oriented crystal domains in resulting materials [Fig. 6(e)].[28] Also, these bond formations in this methodology occur under drastically lower pressure than the typical nanocrystal fusion process (less than 1 GPa vs. 8–10 GPa), owing to the high-surface energy of the bare nanocrystal core.[28] In addition, bare nanocrystals can bypass the surfactant dissociation process, which is another factor in achieving nanocrystal fusion under relatively low pressure.[28] Due to the low sintering pressure, the nanocrystal coining process can be scaled up readily, as approximately 1 GPa can be generated with a typical piston-cylinder, press machine, and other powder metallurgy techniques.[30]

## High-pressure phase materials

The phases of materials are governed by thermodynamics, but there are some exceptions. An example is supercooled water, which can remain in a liquid state below its freezing temperature as low as − 83°C.[60,61] Such materials are in a metastable state and are stabilized kinetically. Solid materials with high-pressure phases at ambient pressure are also metastable materials.[17] Although materials with high-pressure phases have an energetic penalty and are thermodynamically unfavorable,[8,10] some reports have documented that nanocrystals can hold a high-pressure phase even after the applied pressure is released. Early work by Alivisatos' group suggested that a small amount of high-pressure phase of CdSe was detected after releasing a pressure of about 10 GPa [Fig. 2(b)].[37] A study using PbS nanocrystal superlattices by Wang et al. also reported 33–37% preservation of high-pressure phase (orthorhombic-base structure) after releasing pressure.[40] However, the mechanisms behind this phenomenon have not been fully clarified until a recent report by the Cao group in 2022.[17]

Cao et al. demonstrated that preserving high-pressure phases at ambient pressure can be achieved with adequate surface engineering on nanocrystals.[17] Figure 7(a) shows the schematics of this procedure. When nanocrystal superlattices are put under high pressure, the superlattices become smaller and distorted, and their crystal structures change to a high-pressure phase. During this transformation process, the cores of the nanocrystals can touch each other [highlighted in red and yellow atoms in the models in Fig. 7(b and d)], leading to core–core physical touching-network formation spreading throughout the superlattices.[17] The nanocrystal network would retain after releasing the pressure, which provides a huge activation energy, making the metastable high-pressure phase at ambient pressure stable enough to survive for at least 7 years.[17] This method can be robustly applied to CdSe, CdSe@CdS, and CdS nanomaterials with a variety of shapes and structures.[17]

### The significance

Many materials with high-pressure phases exhibit desirable functions such as superconductivity, fluorescence, mechanical properties, etc.[6–12] This methodology can potentially bring these fundamental studies under high pressure into real technologies without holding externally-applied pressure in the materials. In addition, these metastable phase materials possess a high-energy state, which could exhibit distinct chemical reactivity or catalytic properties.[7,8]

Moreover, this process is scalable as it causes irreversible structural changes at the atomic level. While a single pressing process using a DAC can handle only a relatively small amount of sample, multiple pressing processes or pressurizing with a larger pressure cell, such as multi-anvil cells, can enable the production of large-scale metastable materials.

### The surfactant

This methodology relies on the surfactants of nanocrystals in multiple roles, and both qualitative and quantitative controls on surfactants are necessary for the successful preservation of high-pressure phases.[17] Figure 7(c) shows WAXS (wide-angle X-ray scattering) and SAXS patterns collected during compression and decompression at different pressures for superlattices of 4.8-nm CdSe nanocrystals with three different surface states; the CdSe nanocrystals were functionalized with octylamine of (i) 92% surface coverage, (ii) 62% surface coverage, and (iii) capped with a mixture of octylamine and cetyltrimethyl ammonium bromide (CTAB) (with a molar ratio of 5:1) of 63% surface coverage.[17] The WAXS patterns after releasing pressure in (i), (ii), and (iii) show 0%, 50–60%, and 100% of high-pressure phase rock-salt structure was preserved, respectively, demonstrating the ligand-tailorable reversibility in superlattices.[17] The requirements for surfactants to achieve high-pressure phase preservation are as follows. Firstly, the surfactants assist in the formation of the nanocrystal-network architecture. For this reason, the molecular length must be adequate (c.a., 2 nm), and the density must be high enough (i.e., more than 40%).[17] At the

same time, surfactant molecules should not prevent nanocrystal cores from touching each other under high pressure. Therefore, molecules that are too long, too densely packed on the surface (over 80%), and too strongly bound to nanocrystal cores are not suitable.[17] Successful nanocrystal-network formation can vary depending on the nanocrystal components. For example, CdS nanocrystals can preserve the high-pressure phase relatively easily with 95% coverage of octylamine, while CdSe nanocrystals require special treatments to weaken the binding energy by adding CTAB to the surface.[17]

### *The reactions at the surface of nanocrystals*

Pressurized nanocrystal aggregates form a core–core physical touching network. Computer model studies [Fig. 7(d, e)], high-resolution TEM images, conductivity measurements, and structural characterization using X-ray scattering suggest that there are physical associations between nanocrystals but not through chemical bond formations that can fuse nanocrystals.[17] Direct observation of the interface reaction between nanocrystals is not possible, however, the association between nanocrystals provides energetic stability to nanocrystals holding high-pressure phase at least 1.3 eV per particle for the rock-salt -to- zinc-blend solid phase transformation.[62] A deeper understanding of the nature of the nanocrystal network could lead to further generalizations of high-pressure phase preservations.

## Perspectives and challenges

We have introduced state-of-the-art materials created by high-pressure nanochemistry, emphasizing the importance of the surface.[16] There are several foreseeable advances in the extension of these achievements. For grain-boundary materials, further intricate grain-boundary designs (such as solid dispersant composite materials)[58,59] could be achieved using suitable starting nanocrystals such as core–shell nanocrystals, hybrid nanocrystals, multicomponent nanocrystals.[63] Materials molding designed for specific applications could be achieved by combining existing techniques such as 3D or inkjet printing[64,65] using nanocrystal-dispersion as the ink and powder metallurgy techniques.[30] Another promising avenue is high-pressure chemical reactions between nanocrystals. Alloying processes,[48] solid–solid metathesis,[66] and reactions at the surface and interface[67] could be subjected to high-pressure driven reactions. Taking advantage of the ability to tune many important parameters leading to tunable reactivity, such as nanocrystal size, surface, and components, we can expect to explore solid state chemistry that would lead to high efficiency and novel reactions.

To achieve these exciting goals, a deeper understanding and quantitative analysis of the nanocrystal surface is critical.[68] However, assessing the surface is challenging due to the lack of direct observation techniques. Fortunately, recent technological advancements have enabled us to investigate nanocrystal surfaces in greater detail than ever. This section introduces experimental and cutting-edge characterization techniques for accessing nanocrystal surfaces, which could be helpful for further advancing our understanding about high-pressure surface nanochemistry. Table I summarizes these methods, and we explain each method below.

### *Dispersion experiments*

Dispersion experiments are a common and easy method for checking if nanocrystals retain good surfactant states in aggregates.[26] In this experiment, pressurized nanocrystal aggregates are exposed to good solvents. For typical nanocrystals capped by hydrocarbon-chain-based molecules, good solvents are non-polar solvents like toluene, hexane, and cyclohexane. If only van der Waals bonds are formed between nanocrystal aggregates and the nanocrystals still have their original surfactants, the nanocrystals will form a stable dispersion. However, if stronger chemical bonds, such as metal bonds or ionic bonds, are formed between nanocrystals or if surfactants are

**Table I.** Proposed characterization methods for surface of nanocrystals and grain-boundary conditions for high-pressure experiments.

| Methods | Pros | Cons |
|---|---|---|
| Dispersion experiment | Easy experiments | No quantitative data |
| Advanced TEM | Accurate and direct observation of atomic structures of NC inorganic cores | Expensive instruments. Organic surfactant cannot be detected |
| Conductivity Measurement | Evidence of nanocrystal network. *In-situ* measurement in a DAC. Non-destructive | Semi-quantitative information |
| Single-crystal X-ray diffraction | Accurate and direct observation of atomic structures of both NC cores and surfactants. *In-situ* measurements in a DAC | Sample preparation (single crystals) could be challenging for NCSLs |
| Neutron scattering | Simultaneous characterization of both nanocrystal surface and core. *In-situ* measurements in a DAC | Synchrotron light source is needed |
| FTIR and Raman spectrum | Can monitor the molecular transformation. *In-situ* measurements in a DAC | Semi-quantitative information |
| Weight analysis (TGA and ICP) | Feasibility. Quantitative analysis. Well-established methodology | Sample will be destroyed |
| XES and XAS | Detailed atomic information. *In-situ* measurements in a DAC | Synchrotron light source is needed |

dissociated from nanocrystal cores during the pressurizing process, a good solvent cannot disperse the nanocrystals.

## Advanced transmission electron microscopy

TEM has witnessed drastic advancements in the last decade, enabling ultrahigh-resolution characterizations of nanomaterials, including complete 3D atomic tomography and grain-boundary conditions with state-of-the-art TEMs.[55,69–71] These techniques can help us to iterate nanocrystal surface behaviors.[55,69,70] The Miao group has developed a 3D atomic tomography technique with an accuracy of the atomic resolution, enabling precise determination of atomic positions and leading to a better understanding of nanomaterials' surface.[55] The Ikuhara group has reported a series of microscopic techniques to visualize grain-boundary conditions in condensed materials.[69,70] While the characterization of organic surfactants has remained challenging,[71] cryo-TEMs, which have been used to successfully visualized soft materials,[72] would enable direct observation of total colloidal nanocrystal structures including inorganic cores and organic surfactants.

## Conductivity measurements

Conductivity measurements can determine whether nanocrystals' inorganic cores have connections throughout the samples.[17,28] Typically, aggregated nanocrystals exhibit high electrical resistivity ($<0.01$ S/m) due to insulating organic molecules that block electrons from passing through.[28] However, when inorganic nanocrystal cores (e.g., metals and semiconductors) form connections, the connections provide electron pathways, resulting in highly enhanced conductivity ($>10^3$ S/m) even when the materials are embedded with organic surfactant molecules.[28] Conductivity measurements cannot provide detailed information on the bond nature, but they can detect physical touch between nanocrystals in the pressurized state without disassembling the nanocrystal aggregate. In addition, *in situ* conductivity measurements during the pressurizing process with a DAC have been well studied,[73] allowing real-time observations of nanocrystal formation networks.

## Single-crystal X-ray crystallography

Applying single-crystal X-ray crystallography to colloidal nanomaterials visualizes all atomic positions of materials. Jin reported a series of gold clusters that were crystallized in a single crystal, and the single-crystal X-ray crystallography measurements were taken to illustrate all accurate atomic positions of the surfactants and cluster cores.[74] Importantly, single-crystal X-ray crystallography can be equipped with a DAC, allowing for *in-situ* high-pressure experiments with monitoring the pressure response.[75] While it is an ultimately powerful technique to make whole structural information available to scientists, sample preparation with high structural uniformity and maintenance of single crystallinity under pressure will be key requirements for successful measurements of this kind.[76]

## Neutron scattering

Small-angle neutron scattering has been widely used to characterize biomolecules and self-assemblies of organic molecules.[77] Neutron scattering can take advantage of the large difference in scattering cross-sections between hydrogen and deuterium, making it possible to highlight organic surfactants using contrast variation when solvent or ligand are replaced with deuterium-based substituents.[78,79] Recently, researchers have applied this technique to successfully visualize surfactant molecules on nanocrystals. Stellacci et al. demonstrated the 3D visualization of gold nanocrystals and their surfactant profiles were clearly proven from the scattering spectrum and spectrum fitting.[78] Neutron scattering is also readily equipped with DAC,[80] which enables simultaneous *in-situ* measurements of nanocrystal cores and surfactants in response to applied pressure.[81]

## Fourier transfer infra red (FTIR) and Raman spectroscopy

FTIR and Raman spectroscopies are commonly used to characterize nanocrystal surfaces and can be equipped with a DAC for *in-situ* measurements.[27,73] While both techniques are typically considered semi-quantitative and may make it difficult to track the movement of surfactant molecules on or away from nanocrystals, they offer the ability to investigate the molecular state of the surfactant assessing how they react under high pressure when surfactant molecules are reactive in pressure experiments.[73] For example, inorganic clusters like $Cd_2Se_3$ clusters can be turned into CdSe crystals under high pressure and should show high reactivity. By exploring these reactions, we may be able to establish new pressure-driven chemical reactions.

## Thermal gravitational analysis and elemental analysis

One of the most commonly used experimental techniques to quantify the amount of surface area is to determine the weights of surfactants and nanocrystal cores separately using thermal gravitational analysis (TGA) or elemental analysis such as inductively coupled plasma mass spectrometry (ICP-MS).[19] The procedure is, provided that nanocrystals are highly uniform and the total surface area can be calculated, we can obtain the surface density by dividing the surfactant amount by the surface area. Then, the weight ratio between organic surfactants and nanocrystal cores is determined, leading to the determination of the ligand density.[68] Subsequently, we can calculate the surface coverage by dividing the density by the density of a 100% coverage ratio, which was obtained from previous experiments and simulations and is typically arbitrarily 5 molecules/nm$^2$.[28] In TGA, the instruments heat samples and measure weight change during the heating process. Typically, organic surfactants burn at 250–600°C while inorganic nanocrystal cores remain.[17] Similarly, quantitative elemental analysis such as ICP-MS can determine the organic–inorganic weight ratio.

### *X-ray emission and absorption spectroscopy*[24,82]

X-ray emission and absorption spectroscopies are highly sensitive characterization techniques using absorption edges of certain elements, providing element-specific structural information. These techniques are used to characterize the surface state of nanocrystals.[82] A review paper by Shen and Mao comprehensively summarized high-pressure X-ray emission and absorption spectroscopies.[24]

## Coda

To conclude this perspective paper on the promising research field, we highlight important research about quasicrystal meteorites. In 2016, a group led by Steinhart discovered a meteorite containing an aluminum-based quasicrystal alloy.[83] Quasicrystals were first discovered and conceptualized by Dan Shechtman in 1984 in a Fe–Mn alloy,[84] which revolutionized the field of crystallography and brought him the Nobel Chemistry award in 2011. The quasicrystal-containing meteorites found by Steinhart formed 4.6 billion years ago in the Solar nebula.[85] Subsequent work on these naturally formed quasicrystals revealed that they were kinetically formed under high-pressure during meteorite collisions.[85,86] This is just one example of many interesting pressure-driven reactions that occur in nature long before human discovery. In other recent research, scientists found a diamond in a meteorite,[87] while in another study, insights about the inner mantle core were obtained through DAC experiments.[3] Our world was created through the art of pressure, and high-pressure surface nanochemistry can mimic reactions at these geological events.[2,88]

All chemical reactions, either in the lab or in nature, start with a physical interaction between molecules, making it natural to understand that the surface is the primal place to study the reactions of nanocrystals. Therefore, while this perspective paper focuses on the impact on materials science, this topic should provide important insight to other relevant research areas, such as geology, and mechanochemistry. By overcoming the challenges discussed in this article, this research topic could potentially realize the promise to greatly "impact" the entire scientific field.

## Data availability

Not applicable.

## Code availability

Not applicable.

## Declarations

### Conflict of interest

There is no conflict of interest.

## Ethical approval

Not applicable.

## Consent to participate

Not applicable.

## Consent for publication

Not applicable.

## References


1. K. Luo et al., Coherent interfaces govern direct transformation from graphite to diamond. Nature **607**, 486 (2022)
2. Y.-H. Li, G. De, *A compendium of geochemistry: from solar nebula to the human brain* (Princeton University Press, Princeton, 2022)
3. B. Ko et al., Water-induced diamond formation at earth's core–mantle boundary. Geophys. Res. Lett. (2022). https://doi.org/10.1029/2022GL098271
4. Z.W. Ma et al., Pressure-induced emission of cesium lead halide perovskite nanocrystals. Nat. Commun. (2018). https://doi.org/10.1038/s41467-018-06840-8
5. Q. Li et al., Pressure-induced remarkable enhancement of self-trapped exciton emission in one-dimensional CsCu2I3 with tetrahedral units. J. Am. Chem. Soc. **142**, 1786–1791 (2020)
6. J. Lei et al., Synthesis and high-pressure mechanical properties of superhard rhenium/tungsten diboride nanocrystals. ACS Nano **13**, 10036–10048 (2019)
7. Z.M. Xia, Y. Yin, J. Li, H. Xiao, Single-atom catalysis enabled by high-energy metastable structures. Chem. Sci. **14**, 2631–2639 (2023)
8. H.K. Mao, C. Ji, B. Li, G. Liu, E. Gregoryanz, Extreme energetic materials at ultrahigh pressures. Eng. Proc. **6**, 976–980 (2020)
9. Y. Zhou, Z.Y. Dong, W.P. Hsieh, A.F. Goncharov, X.J. Chen, Thermal conductivity of materials under pressure. Nat. Rev. Phys. **4**, 319–335 (2022)
10. L.J. Zhang, Y.C. Wang, J. Lv, Y.M. Ma, Materials discovery at high pressures. Nat. Rev. Mater. (2017). https://doi.org/10.1038/natrevmats.2017.5
11. A.P. Drozdov et al., Superconductivity at 250 K in lanthanum hydride under high pressures. Nature **569**, 528 (2019)
12. L.Z. Deng et al., Pressure-induced high-temperature superconductivity retained without pressure in FeSe single crystals. Proc. Natl. Acad. Sci. USA (2021). https://doi.org/10.1073/pnas.2108938118
13. W. Grochala, R. Hoffmann, J. Feng, N.W. Ashcroft, The chemical imagination at work in very tight places. Angew. Chem. Int. Ed. **46**, 3620–3642 (2007)
14. J.J. Shephard et al., Covalent bond shortening and distortion induced by pressurization of thorium, uranium, and neptunium tetrakis aryloxides. Nat. Commun. (2022). https://doi.org/10.1038/s41467-022-33459-7
15. J.M. Sperling et al., Compression of curium pyrrolidine-dithiocarbamate enhances covalency. Nature **583**, 396 (2020)
16. F. Bai, K. Bian, X. Huang, Z. Wang, H. Fan, Pressure induced nanoparticle phase behavior, property, and applications. Chem. Rev. **119**, 7673–7717 (2019)
17. T.Y. Xiao et al., Nanocrystals with metastable high-pressure phases under ambient conditions. Science **377**, 870–874 (2022)
18. T.H. Yang, Y.F. Shi, A. Janssen, Y.N. Xia, Surface capping agents and their roles in shape-controlled synthesis of colloidal metal nanocrystals. Angew. Chem. Int. Ed. **59**, 15378–15401 (2020)
19. M.A. Boles, D. Ling, T. Hyeon, D.V. Talapin, The surface science of nanocrystals. Nat. Mater. **15**, 141–153 (2016)
20. A. Heuer-Jungemann et al., The role of ligands in the chemical synthesis and applications of inorganic nanoparticles. Chem. Rev. **119**, 4819–4880 (2019)

21. W. Wang et al., Colloidal inorganic ligand-capped nanocrystals: fundamentals, status, and insights into advanced functional nanodevices. Chem. Rev. **122**, 4091–4162 (2022)
22. A. Nag et al., Metal-free inorganic ligands for colloidal nanocrystals: $S_2$-, HS-, $Se_2$-, HSe-, $Te_2$-, HTe-, $TeS_{32}$-, OH-, and $NH_2$- as surface ligands. J. Am. Chem. Soc. **133**, 10612–10620 (2011)
23. Z.W. Wang et al., Integrating in situ high pressure small and wide angle synchrotron x-ray scattering for exploiting new physics of nanoparticle supercrystals. Rev. Sci. Instrum. (2010). https://doi.org/10.1063/1.3480558
24. G.Y. Shen, H.K. Mao, High-pressure studies with x-rays using diamond anvil cells. Rep Prog Phys **80**, 1–53 (2017)
25. H.K. Mao, J. Xu, P.M. Bell, Calibration of the ruby pressure gauge to 800-Kbar under quasi-hydrostatic conditions. J. Geophys. Res. Solid **91**, 4673–4676 (1986)
26. Y. Nagaoka et al., Nanocube superlattices of cesium lead bromide perovskites and pressure-induced phase transformations at atomic and mesoscale levels. Adv. Mater. **29**, 1606666 (2017)
27. H.J. Yang et al., Access and capture of layered double perovskite polytypic phase through high-pressure engineering. J. Phys. Chem. C **127**, 2407 (2023)
28. Y. Nagaoka et al., Bulk grain-boundary materials from nanocrystals. Chem-Us **7**, 509–525 (2021)
29. J. Zhang, B.L. Liu, R.Q. Lu, Q.F. Yang, Q.M. Dai, Study on oil film characteristics of piston-cylinder pair of ultra-high pressure axial piston pump. Processes **8**, 68 (2020)
30. O.V. Kharissova, L.M. Torres-Martínez, B.I. Kharisov, *Handbook of nanomaterials and nanocomposites for energy and environmental applications*, 1st edn. (Springer International Publishing, Cham, 2021)
31. D.W. Jiang, M. Cao, X.T. Zhang, Y. Gao, Y.H. Han, Pressure evolution in a diamond anvil cell without a pressure medium. J. Appl. Phys. **131**, 125904 (2022)
32. N.E. Dowling, S.L. Kampe, M.V. Kral, *Mechanical behavior of materials* (Global Edition, Pearson, 2020)
33. W. Li, H. Fan, J. Li, Deviatoric stress-driven fusion of nanoparticle superlattices. Nano Lett. **14**, 4951–4958 (2014)
34. R. Mandal, C. Casert, P. Sollich, Robust prediction of force chains in jammed solids using graph neural networks. Nat. Commun. (2022). https://doi.org/10.1038/s41467-022-31732-3
35. S. Ostojic, E. Somfai, B. Nienhuis, Scale invariance and universality of force networks in static granular matter. Nature **439**, 828–830 (2006)
36. J.W. Xiao, B. Wen, R. Melnik, Y. Kawazoe, X.Y. Zhang, Phase transformation of cadmium sulfide under high temperature and high pressure conditions. Phys. Chem. Chem. Phys. **16**, 14899–14904 (2014)
37. S.H. Tolbert, A.P. Alivisatos, Size dependence of a first-order solid-solid phase-transition—the wurtzite to rock-salt transformation in Cdse nanocrystals. Science **265**, 373–376 (1994)
38. K. Jacobs, J. Wickham, A.P. Alivisatos, Threshold size for ambient metastability of rocksalt CdSe nanocrystals. J. Phys. Chem. B **106**, 3759–3762 (2002)
39. S.H. Tolbert, A.P. Alivisatos, High-pressure structural transformations in semiconductor nanocrystals. Annu. Rev. Phys. Chem. **46**, 595–625 (1995)
40. T. Wang et al., Pressure processing of nanocube assemblies toward harvesting of a metastable PbS phase. Adv. Mater. **27**, 4544–4549 (2015)
41. B.S. Li et al., Pressure compression of CdSe nanoparticles into luminescent nanowires. Sci. Adv. (2017). https://doi.org/10.1126/sciadv.1602916
42. H. Zhu et al., Pressure-enabled synthesis of hetero-dimers and hetero-rods through intraparticle coalescence and interparticle fusion of quantum-dot-au satellite nanocrystals. J. Am. Chem. Soc. **139**, 8408–8411 (2017)
43. T.T. Yin et al., High-pressure-induced comminution and recrystallization of $CH_3NH_3PbBr_3$ nanocrystals as large thin nanoplates. Adv. Mater. **30**, 1705017 (2018)
44. H.M. Wu et al., Pressure-driven assembly of spherical nanoparticles and formation of 1D-nanostructure arrays. Angew. Chem. Int. Ed. **49**, 8431–8434 (2010)
45. H. Wu et al., Nanostructured gold architectures formed through high pressure-driven sintering of spherical nanoparticle arrays. J. Am. Chem. Soc. **132**, 12826–12828 (2010)
46. W. Baek et al., Recent advances and prospects in colloidal nanomaterials. JACS Au **1**, 1849–1859 (2021)
47. A.K. Pearce, T.R. Wilks, M.C. Arno, R.K. O'Reilly, Synthesis and applications of anisotropic nanoparticles with precisely defined dimensions. Nat. Rev. Chem. **5**, 21–45 (2021)
48. C. Gadiyar et al., Nanocrystals as precursors in solid-state reactions for size- and shape-controlled polyelemental nanomaterials. J. Am. Chem. Soc. **142**, 15931–15940 (2020)
49. T. Burgi, Properties of the gold-sulphur interface: from self-assembled monolayers to clusters. Nanoscale **7**, 15553–15567 (2015)
50. Z.W. Wang et al., Deviatoric stress driven formation of large single-crystal PbS nanosheet from nanoparticles and in situ monitoring of oriented attachment. J. Am. Chem. Soc. **133**, 14484–14487 (2011)
51. P. Podsiadlo et al., High-pressure structural stability and elasticity of supercrystals self-assembled from nanocrystals. Nano Lett. **11**, 579–588 (2011)
52. B. Li et al., Stress-induced phase transformation and optical coupling of silver nanoparticle superlattices into mechanically stable nanowires. Nat. Commun. **5**, 4179 (2014)
53. L.Y. Meng et al., Pressure induced assembly and coalescence of lead chalcogenide nanocrystals. J. Am. Chem. Soc. **143**, 2688–2693 (2021)
54. T. Watanabe, Grain boundary engineering: historical perspective and future prospects. J. Mater. Sci. **46**, 4095–4115 (2011)
55. Y.K. Yuan et al., Three-dimensional atomic packing in amorphous solids with liquid-like structure. Nat. Mater. **21**, 95 (2022)
56. Y. Liu et al., Surfactant-induced postsynthetic modulation of Pd nanoparticle crystallinity. Nano Lett. **11**, 1614–1617 (2011)
57. J. De Roo, Chemical considerations for colloidal nanocrystal synthesis. Chem. Mater. **34**, 5766–5779 (2022)
58. Q.T. Zhang et al., Achieving ultralow lattice thermal conductivity and high thermoelectric performance in GeTe alloys via introducing $Cu_2Te$ nanocrystals and resonant level doping. ACS Nano **15**, 19345–19356 (2021)
59. Y. Liu et al., Wide-bandgap perovskite quantum dots in perovskite matrix for sky-blue light-emitting diodes. J. Am. Chem. Soc. **144**, 4009–4016 (2022)
60. G.O. Gomes, H.E. Stanley, M. de Souza, Enhanced gruneisen parameter in supercooled water. Sci. Rep. (2019). https://doi.org/10.1038/s41598-019-48353-4
61. L. Kringle, W.A. Thornley, B.D. Kay, G.A. Kimmel, Reversible structural transformations in supercooled liquid water from 135 to 245 K. Science **369**, 1490 (2020)
62. M. Grunwald, K. Lutker, A.P. Alivisatos, E. Rabani, P.L. Geissler, Metastability in pressure-induced structural transformations of CdSe/ZnS core/shell nanocrystals. Nano Lett. **13**, 1367–1372 (2013)
63. C.R. McCormick, R.R. Katzbaer, B.C. Steimle, R.E. Schaak, Combinatorial cation exchange for the discovery and rational synthesis of heterostructured nanorods. Nat. Synth. **2**, 152–161 (2023)
64. S.F. Liu et al., 3D nanoprinting of semiconductor quantum dots by photoexcitation-induced chemical bonding. Science **377**, 1112–1116 (2022)
65. L.R. Meza et al., Resilient 3D hierarchical architected metamaterials. Proc. Natl. Acad. Sci. USA **112**, 11502–11507 (2015)
66. L. Lei, L.L. Zhang, Recent advance in high-pressure solid-state metathesis reactions. Matter. Radiat. Extrem. **3**, 95–103 (2018)
67. J.B. Cui et al., Neck barrier engineering in quantum dot dimer molecules via intraparticle ripening. J. Am. Chem. Soc. **143**, 19816–19823 (2021)
68. A.M. Smith, K.A. Johnston, S.E. Crawford, L.E. Marbella, J.E. Millstone, Ligand density quantification on colloidal inorganic nanoparticles. Analyst **142**, 11–29 (2017)
69. J.K. Wei et al., Direct imaging of atomistic grain boundary migration. Nat. Mater. **20**, 951 (2021)
70. J.K. Wei, B. Feng, E. Tochigi, N. Shibata, Y. Ikuhara, Direct imaging of the disconnection climb mediated point defects absorption by a grain boundary. Nat. Commun. (2022). https://doi.org/10.1038/s41467-022-29162-2

71. M.G. Panthani et al., Graphene-supported high-resolution TEM and STEM imaging of silicon nanocrystals and their capping ligands. J. Phys. Chem. C **116**, 22463–22468 (2012)
72. J. Watt, D.L. Huber, P.L. Stewart, Soft matter and nanomaterials characterization by cryogenic transmission electron microscopy. MRS Bull. **44**, 942–948 (2019)
73. R. Matsumoto et al., High-pressure synthesis of superconducting Sn3S4 using a diamond anvil cell with a boron-doped diamond heater. Inorg. Chem. **61**, 4476–4483 (2022)
74. Y.W. Li, R.C. Jin, Seeing ligands on nanoclusters and in their assemblies by X-ray crystallography: atomically precise nanochemistry and beyond. J. Am. Chem. Soc. **142**, 13627–13644 (2020)
75. E.Z. Eikeland et al., Single-crystal high-pressure X-ray diffraction study of host structure compression in clathrates of Dianin's compound. Cryst. Growth Des. **20**, 4092–4099 (2020)
76. Y. Nagaoka et al., Superstructures generated from truncated tetrahedral quantum dots. Nature **561**, 378 (2018)
77. J.L. Marx, Neutron-scattering—new look at biological molecules. Science **198**, 481–483 (1977)
78. Z. Luo et al., Quantitative 3D determination of self-assembled structures on nanoparticles using small angle neutron scattering. Nat. Commun. (2018). https://doi.org/10.1038/s41467-018-03699-7
79. H.D. Mertens, D.I. Svergun, Structural characterization of proteins and complexes using small-angle X-ray solution scattering. J. Struct. Biol. **172**, 128–141 (2010)
80. J. Binns, K.V. Kamenev, G.J. McIntyre, S.A. Moggach, S. Parsons, Use of a miniature diamond-anvil cell in high-pressure single-crystal neutron Laue diffraction. IUCrj **3**, 168–179 (2016)
81. A. Grzechnik, M. Meven, C. Paulmann, K. Friese, Combined X-ray and neutron single-crystal diffraction in diamond anvil cells. J. Appl. Crystallogr. **53**, 9–14 (2020)
82. J.L. Stein et al., Probing surface defects of InP quantum dots using phosphorus K alpha and K beta X-ray emission spectroscopy. Chem. Mater. **30**, 6377–6388 (2018)
83. L. Bindi et al., Natural quasicrystal with decagonal symmetry. Sci. Rep. **5**, 9111 (2015)
84. D. Shechtman, I. Blech, D. Gratias, J.W. Cahn, Metallic phase with long-range orientational order and no translational symmetry. Phys. Rev. Lett. **53**, 1951–1953 (1984)
85. M. Miyahara, N. Tomioka, L. Bindi, Natural and experimental high-pressure, shock-produced terrestrial and extraterrestrial materials. Progress Earth Planet. Sci. (2021). https://doi.org/10.1186/s40645-021-00451-6
86. P.D. Asimow et al., Shock synthesis of quasicrystals with implications for their origin in asteroid collisions. Proc. Natl. Acad. Sci. USA **113**, 7077–7081 (2016)
87. A.G. Tomkins et al., Sequential lonsdaleite to diamond formation in ureilite meteorites via in situ chemical fluid/vapor deposition. Proc. Natl. Acad. Sci. USA **119**, e2208814119 (2022)
88. G. Sposito et al., Surface geochemistry of the clay minerals. Proc. Natl. Acad. Sci. USA **96**, 3358–3364 (1999)